

# Effects of Mask Misalignment and Wafer Misorientation on Silicon V-Groove Etching

Songsheng Tan, Robert Boudreau and Michael L. Reed<sup>§\*</sup>

Packaging and Assembly Core Technology, Corning Inc.  
Corning, NY 14831 USA<sup>\*</sup>

<sup>§</sup>Department of Electrical and Computer Engineering, University of Virginia  
PO Box 400743, Charlottesville, VA 22904-4743 USA

(Received October 10, 2003; accepted March 1, 2003)

**Key words:** anisotropic, silicon etching, micromachining, MEMS, V-groove, misaligned

We present an analysis of nonuniform mask undercut which occurs during fabrication of V-grooves by anisotropic etching of silicon. Mask undercut is known to be highly sensitive to alignment of the etch window with the  $\langle 110 \rangle$  crystal direction. We show that the configuration of the mask patterns defining the end of the groove has a strong influence on the uniformity of the mask undercut and whether the V-groove sidewalls are true  $\{111\}$  or near  $\{111\}$  planes. Mask patterns with closed ends result in V-grooves whose sides are true (111) planes after long etches; open-ended mask patterns result in V-grooves with near (111) planes. These results can be explained in terms of step generation and movement during the etching process. Displacements of the V-groove centerline as a function of mask misalignment angle and wafer surface misorientation are calculated.

## 1. Introduction

Anisotropic etching of silicon in KOH and other solutions is a widely used technology for bulk micromachining. One application is the precise alignment of fiber optic cables to optical emitters, known as “silicon waferboard” technology.<sup>(1)</sup> This is accomplished by etching a V-groove defined by  $\{111\}$  planes in a (001) silicon wafer, along with pedestals which locate the emitter. The idea is that the fiber will snugly nestle into the V-groove, thus precisely aligning it to the emitter for minimum coupling loss. The V-groove is fabricated by lithographically opening a rectangular area in a masking film such that the long edges of

---

\*Corresponding author

the mask are aligned along  $\langle 110 \rangle$  directions. Because the etch rate of  $\{111\}$  silicon planes is much lower than the etch rate of other crystallographic planes, deep V-grooves can be fabricated with a precisely defined apex angle and well-controlled dimensions.

Knowledge of the behavior of anisotropic etching of  $\{111\}$  and near- $\{111\}$  planes is necessary for fine design and precise control of the V-groove etching. Figure 1 shows a micrograph of a silicon waferboard structure for aligning a fiber cable with a laser. The distance  $\Delta d$  between the alignment pedestal and the V-groove centerline must be controlled to within  $\pm 1 \mu\text{m}$  to ensure adequate coupling of the laser emission into the fiber.<sup>(2)</sup> Various factors affect the accuracy with which this distance can be controlled, including critical dimension control during lithographic definition and etching of the pedestals, alignment accuracy of the V-groove mask patterns, and V-groove anisotropic etch reproducibility. In this paper we discuss the effects of the nature of the mask and its alignment on the V-groove after anisotropic etching.

## 2. Experimental Procedure

Four-inch, (001)-oriented, Czochralski and float-zone silicon wafers, with one side polished and with resistivities ranging from  $10 \Omega\text{-cm}$  to over  $5000 \Omega\text{-cm}$  were used in these experiments. Low-pressure chemical-vapor-deposited silicon nitride was used as the etching mask. Most etching studies were performed with simple V-groove masks aligned to the wafer flat. A prealignment mask was used in experiments requiring precision alignment to better than  $0.05^\circ$ .<sup>(3)</sup> All etching experiments were carried out in an isothermal bath controlled to within  $\pm 0.1^\circ\text{C}$ . The 35% (by weight) aqueous KOH solutions were prepared by diluting commercial "SEMI" grade potassium hydroxide solution (45% by weight) and saturating with 2-propanol. Samples were etched for 3 to 10 hours. After etching, the wafers were observed and images recorded using an Olympus Model BX60M microscope equipped with a Sony color video printer.

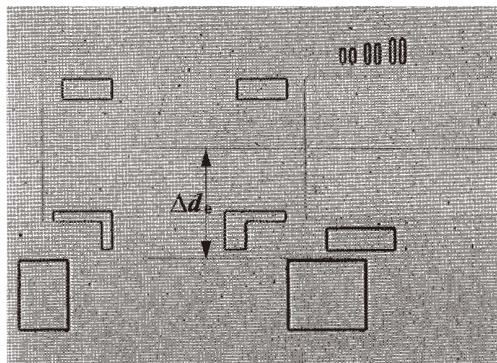


Fig. 1. Micrograph of a silicon waferboard structure for aligning a fiber cable with a laser. The distance  $\Delta d$  between the alignment pedestal and the V-groove centerline must be controlled to within  $\pm 1 \mu\text{m}$  to ensure adequate coupling.

### 3. Results and Discussion

#### 3.1 Effects of mask misalignment on closed-end V-groove etching

The principle of V-groove etching in silicon is that  $\{111\}$  surfaces are attacked at a much lower rate than all other crystal planes in anisotropic etchants. When rectangular strip openings in a silicon nitride mask are aligned along  $\langle 110 \rangle$  directions on a (001) wafer, V-shaped grooves result after anisotropic etching. The lateral sides of the V-grooves are  $\{111\}$  crystal planes which have the lowest etch rate. Depending on the conditions, the etch rate anisotropy between  $\{100\}$  and  $\{111\}$  planes can be as high as 200:1. This permits precise control of the V-groove dimensions, which is necessary for accurate placement of the fiber later in the process.

The mask patterns are aligned parallel or orthogonal to the flat wafer, which is ground to be a  $(1\bar{1}0)$  crystal plane, so that the V-groove axes are in one of the two  $\langle 110 \rangle$  directions in the plane of the wafer surface. Perfect alignment of the mask with the crystal results in ideal V-grooves. The intersections of the V-groove sidewalls with the wafer surface are likewise in the  $\langle 110 \rangle$  direction, resulting in uniform mask undercut along the length of the V-groove. Figure 2 shows the extreme left and right ends of a long closed-end V-groove which was accurately aligned. In this figure, the center rectangular opening is the open area of the silicon nitride. The thin lighter colored area around this rectangle is the overhanging mask film defined by the mask undercut. Note that the mask undercut is perfectly uniform, resulting in a V-groove whose centerline is in the  $[110]$  direction, aligned to both the crystal and to the edges of the mask.

Generally, some amount of misalignment of the mask to the crystal is unavoidable. Figure 3 illustrates a V-groove resulting from a misaligned mask. At the left end the mask undercut of the upper side is less than that of the lower side. At the right end the undercut is opposite, with the upper side more undercut than the lower side. As discussed below, with closed-end mask patterns, long etching results in V-grooves whose sides are still true- $\{111\}$  planes. Therefore, this V-groove is aligned to the crystal planes; that is, the centerline of the V-groove is parallel to the  $[110]$  crystal direction. However, since the mask itself was misaligned to the  $[110]$ , the V-groove is *not* aligned to the mask edges, resulting in the nonuniform mask undercut. The misalignment thus causes a twisting of the V-groove centerline with respect to the mask edges. This twisting will reduce the coupling efficiency between lasers and optical fibers in passive alignment schemes. (This is true

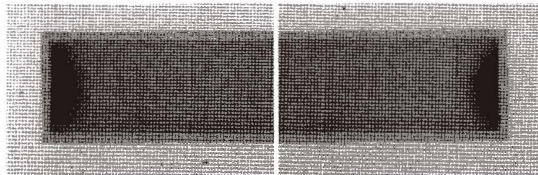


Fig. 2. Micrograph of closed-end V-groove illustrating the undercut resulting from a well-aligned mask. The overhanging edge of the silicon nitride mask is uniform at the extreme left and right ends of the V-groove when the etch mask is well-aligned to a  $\langle 110 \rangle$  direction.

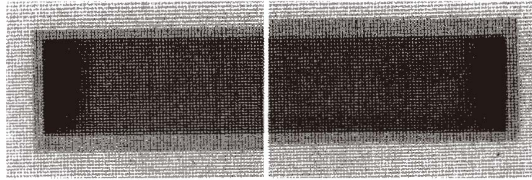


Fig. 3. Photomicrograph of closed-end V-groove with a misaligned mask. The overhang is seen to be nonuniform along the length of the groove. Misalignment of a closed end mask pattern with respect to the  $\langle 110 \rangle$  crystal direction results in a twisting of the etched V-groove with respect to the mask edges. The sidewalls of the V-groove are true  $\{111\}$  planes when the mask pattern has closed ends. The intersections of these sidewalls with the (001) wafer surface are in the true  $\langle 110 \rangle$  directions, so misalignment of the mask is readily apparent.

even if the masking material is stripped, since emitter alignment pedestals are referenced to marks made by the V-groove mask, not the V-groove itself.)

This twisting is centered around the midpoint (along the length) of the V-groove. Laser alignment pedestals, referenced to features on the V-groove mask, will therefore be offset from the groove centerline by an amount  $\Delta d$ . Quantitatively, the laser misalignment is given by

$$\Delta d = \frac{L}{2} \sin \theta \approx \frac{L\theta}{2}, \quad (1)$$

where  $L$  is the V-groove length and  $\theta$  is the misalignment angle in radians. Figure 4 plots the magnitude of the laser offset for small angular misalignments, using a typical V-groove length of 2 mm. We see that the consequences of even slight angular misalignment are serious; a mask rotation of as little as  $0.06^\circ$  results in a laser/fiber shift of  $1 \mu\text{m}$ , sufficient to cause considerable coupling loss.

The results of Fig. 4 are based on the argument that the sidewalls of closed-end V-grooves are  $\{111\}$  crystal planes. This is the case when the etching time is long. In practice, a usable V-groove, whose sides are composed of near- $\{111\}$  planes, can develop in the silicon before this state is reached. (The mechanism responsible for this situation is described in the next section.) As a result, Fig. 4 represents an upper limit on the offset of the laser pedestals.

### 3.2 Effects of mask pattern geometry on V-groove etching

Only a small number of crystal planes are atomically flat. In silicon, this includes the  $\{111\}$  planes, and perhaps the  $\{100\}$  and  $\{110\}$  planes. Etched silicon surfaces, even these planes, are not atomically flat.<sup>(4)</sup> Planes in the vicinity of  $\{111\}$  ("near- $\{111\}$  planes") consist of terraces of true  $\{111\}$  with occasional steps.<sup>(5)</sup> A cross-sectional representation of a near- $\{111\}$  is depicted in Fig. 5. A higher degree of misalignment results in more step sites per unit length.

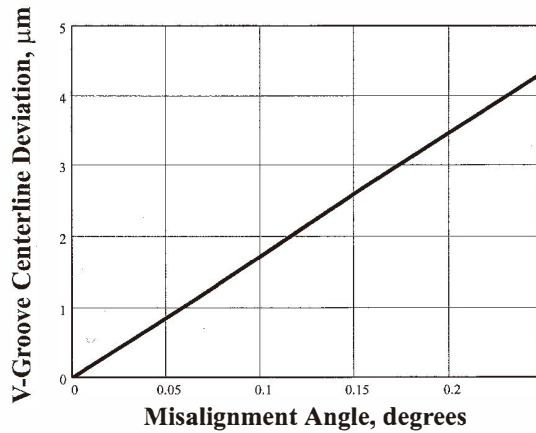


Fig. 4. Displacement of the V-groove center position at one end as a function of mask misalignment angle, for a 2 mm long V-groove. This graph represents the error in positioning a laser relative to a fiber nestled in a V-groove. Even slight misalignments of as little as  $0.06^\circ$  can result in serious coupling losses.

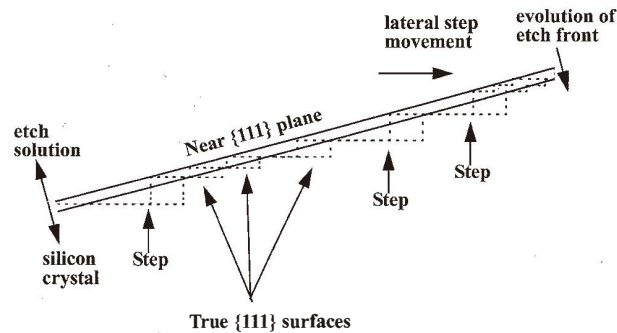


Fig. 5. Schematic of the anisotropic etching mechanism of near  $\{111\}$  planes. The surface is composed of true  $\{111\}$  planes and steps. Etching proceeds by the removal of silicon atoms at the step locations, which results in the lateral motion of steps.

Etching of near- $\{111\}$  planes is thought to proceed by the lateral movement of steps. The energy required to remove an atom at a step is considerably less than that required to remove an atom from an atomically flat, true  $\{111\}$  surface. We can think of the etching of the near- $\{111\}$  in Fig. 5 as the steps sweeping from left to right, which causes the etch front to move parallel to its original position. (This description has been confirmed by scanning tunneling microscope images of etched surfaces.<sup>(6)</sup>) With greater misalignment, there is a larger number of steps, and hence a higher etch rate, as is observed experimentally.<sup>(7)</sup>

Figure 6 shows the region near the corner of an etch cavity on a (110) wafer, where the mask pattern is open at the left (off the edge of the photograph). In this micrograph the upper dark area is the etch cavity; the lower region is the surface of the silicon as seen through the overhanging mask. (On a (110) wafer, the slow-etching {111} planes are perpendicular to the wafer surface and meet each other at a 109.5° angle; this explains the obtuse angle of the planes observed at the right end of the cavity.) We observe a number of steps, indicated by arrows, along the lower sidewall. No steps are seen on the right sidewall. Along the lower edge, new steps are generated at the open left side of the mask pattern. Along the right side, the steps have already been swept out, forming a true {111} surface. Due to the corner, new steps cannot form along the right sidewall except by the energetically unfavorable removal of an atom from the {111} surface.

In closed-end V-grooves with slight angular misalignments, the steps sweep in opposite directions on the upper and lower side faces of the V-groove, Fig. 7. This characteristic step movement on either side of the V-groove will eventually result, after sufficiently long etching, in true {111} planes and nonuniform mask undercut. Larger undercut is seen in areas where a greater number of steps are sweeping through, away from the relevant closed end of the mask. Once the sidewalls become true {111} planes, lateral step movement stops and the etch rate decreases considerably, limited by the (very slow) generation rate of new steps.

However, we observe very different behavior when the ends of the V-groove mask are open. Without a closed end, there is no mechanism to limit the generation of new steps. As etching proceeds, steps are continually generated at the open ends, resulting in a constant sweeping across and a uniform mask undercut along the length of the groove on both edges.

Figure 8 shows two open-end V-grooves, parts of a wagon wheel etch pattern with

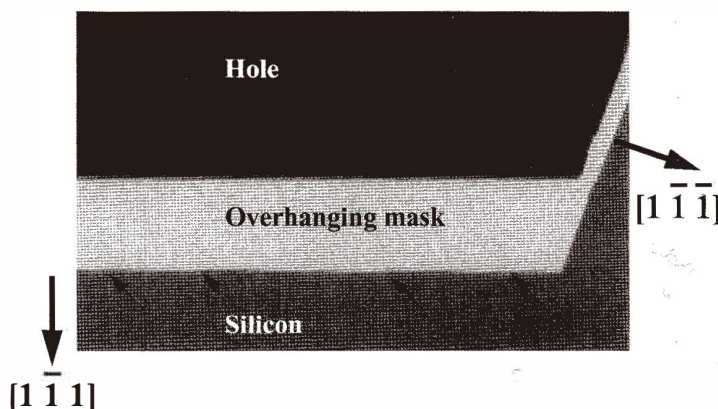


Fig. 6. Micrograph of a V-groove on a (110) wafer. The steps on the lower sidewall are absent on the right sidewall. The etching proceeds by unidirectional lateral movement of steps on the near-{111} planes. Steps on the right edge have already been "swept out"; new steps cannot be generated at the closed corner. Along the lower edge, new steps are generated at the open left side of the mask pattern (off the left side of the photograph) so etching continues. The availability of new steps determines whether or not the V-groove surfaces eventually become true {111} planes.

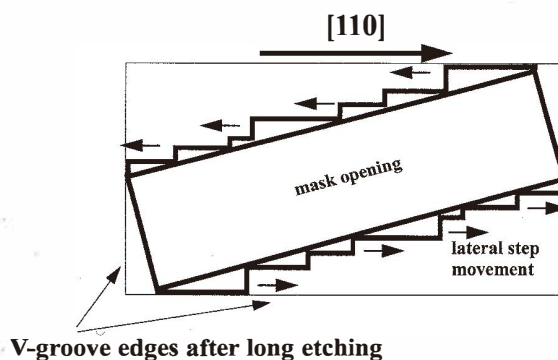


Fig. 7. Evolution of closed-end V-groove with a misaligned mask. Unidirectional step movement in opposite directions on either side will eventually result in a V-groove with true  $\{111\}$  planes, aligned to the true  $[110]$ , and nonuniform mask undercut.

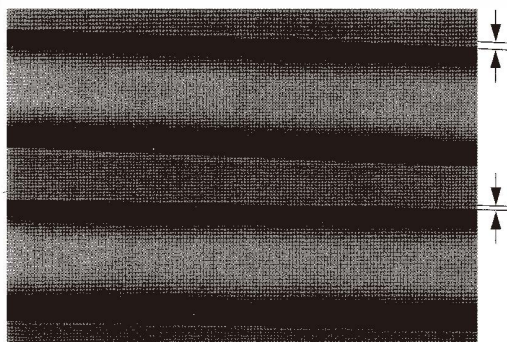


Fig. 8. Micrographs of V-grooves with misaligned open ended mask patterns. The upper groove is misaligned from the  $\langle 110 \rangle$  by  $1^\circ$  more than the lower groove. Unlike the closed-end mask patterns, there is no twisting of the etched V-grooves with respect to the masks. The mask undercut for each pattern is uniform along the length. We also see that the mask undercut, indicated by the dimensional arrows, is greater for the upper (more misaligned) V-groove.

angular increments of  $1^\circ$ . The angular misalignment of the upper V-groove is  $1^\circ$  larger than that of the lower V-groove. There is a corresponding increase in the mask undercut of the upper V-groove; this is to be expected since the greater misalignment creates a higher density of steps and hence a higher etch rate. However, for each groove, the mask undercut is uniform along the length, and is the same on the upper and lower edges. Therefore, the sides of the V-groove remain aligned to the mask, with no twisting of the centerline, although now the V-groove is misaligned to the crystal planes in the silicon. It follows that the sidewalls of the V-groove created with an open-end mask are not true  $\{111\}$  planes.

Figure 9 shows a micrograph of a V-groove created with a mask closed at the left end and open at the right end. On the left end, the undercut is uniform along the length only on the bottom edge. Here, there is a constant supply of steps (which sweep from right to left) available from the open right end. Along the top edge, where the steps sweep in the opposite direction, from left to right, there is only a finite supply of steps owing to the closed mask end on the left. Hence, there is a distinct taper to the mask undercut. On the right end, this effect is not seen because the etch has not progressed sufficiently for the upper sidewall to comprise a true  $\{111\}$  plane. Uniform undercuts are observed on both edges on the right end of the groove because a sufficient number of steps are available to ensure a constant etch rate characteristic of this angular mask misalignment.

Mask misalignment is a primary cause of nonuniform etch undercut. The fundamental etch mechanisms of  $\{111\}$  and near- $\{111\}$  planes give rise to different behaviors for closed- and open-end V-groove masks. Of particular importance is the observation that V-grooves created with closed-end masks will eventually (after long etching) become aligned to the  $\langle 110 \rangle$  crystal direction in the silicon, even when the masks are misaligned, whereas open-end masks will create V-grooves which retain their original mask misalignment. It follows that V-groove twist can be reduced in silicon waferboard applications by using open-ended mask patterns.

### 3.3 Effects of misorientation of the wafer surface from (001)

The preceding discussion is predicated on the assumption that the wafer surface is a true (001) crystal plane. Generally, there will be some slight misorientation of the wafer surface from the true (001) plane; the SEMI standard<sup>(8)</sup> for  $\{100\}$  silicon wafers allows a surface misorientation of up to  $\pm 1.0^\circ$ . With misoriented wafers, the  $\{111\}$  sidewalls of a V-groove will not meet the wafer surface along a  $\langle 110 \rangle$  direction.

Figure 10 illustrates the geometry of V-grooves with aligned and misaligned wafer surfaces. AB and CD are lines defined by the intersection of V-groove sidewalls with the (001) surface plane. These two lines are parallel with each other and are oriented in the

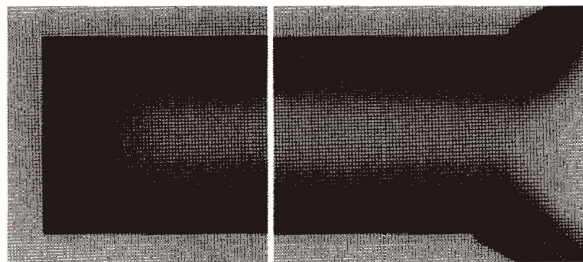


Fig. 9. Micrograph of a V-groove with a mask pattern closed at one end (left) and open at the other (right). There is uniform undercut on both edges at the end of the V-groove where the mask pattern is open. However, the etching near the closed end results in *nonuniform* undercut along one edge (the top), while the other edge exhibits uniform undercut. This can be understood in terms of step generation and movement at each end.



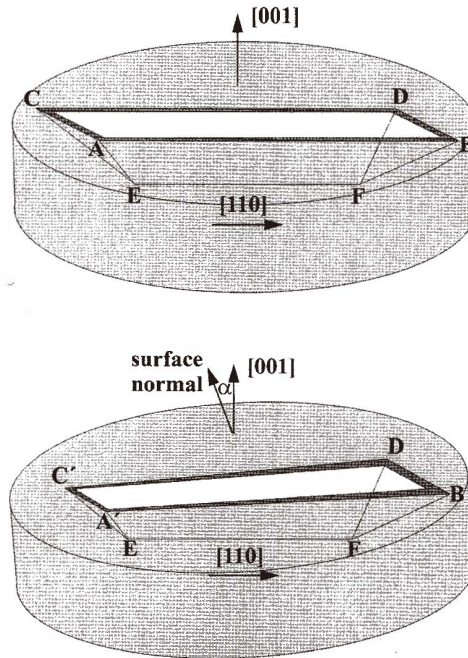


Fig. 10. Schematic of V-grooves etched into wafers with the surface aligned and misaligned from the (001) plane. Top: V-groove in a wafer whose surface is a true (001) plane. The V-groove edges AB and CD are parallel to the V-groove centerline EF; all three lines are parallel to the true [110]. Bottom: V-groove in a wafer whose surface is misoriented from the crystalline (001) by angle  $\alpha$ . The V-groove edges A'B and C'D are not parallel to the V-groove centerline EF or to each other. The centerline EF is still parallel to the true [110]. The V-groove depth and mask undercut are both nonuniform along the length of the structure.

[110] direction. If the wafer surface is tilted off the (001) by a small angle,  $\alpha$ , then the intersections of the V-groove sidewalls with the wafer surface will become A'B and C'D. These lines are not parallel to each other or the [110]. A straightforward calculation shows that the angular divergence of the V-groove edges A'B and C'D is approximately  $1.4\alpha$ .

Figure 11 shows the extreme left and right ends of a long V-groove created with a closed-end mask pattern on a wafer suffering from (001) misorientation, corresponding to the situation outlined in Fig. 11. As before, the two inside lines are the V-groove mask edges, which are parallel to each other. The outside lines are the intersections of the V-groove sidewalls with the wafer surface. We see that these lines are not parallel to each other, or with the V-groove mask edges. There is considerably more mask undercut at the right end of the groove. Because the etch depth is directly proportional to the mask undercut, this means that the fully etched V-groove does not have a uniform depth along its length; the groove is deeper and wider at the right end. If this groove were used for fiber

alignment, the fiber axis would not be parallel to the wafer surface.

Because the wafer flat is generally imperfectly aligned to the crystal, it is common practice to etch a V-groove in the wafer to use for subsequent mask alignments. A V-groove defined by a closed-end mask pattern will comprise faces with true  $\{111\}$  planes and a true  $\langle 110 \rangle$  axis. This "alignment" V-groove defines three lines each of which could be used to orient subsequent masks: the upper edge (where the face meets the surface), the lower edge, and the centerline. Typically, one of the edges will be used because the V-groove centerline is well out of the depth of focus of the alignment tool. In the case of a wafer whose surface is close to the (001), this does not present a problem, as the two edges and centerline of the V-groove are parallel. However, when the wafer surface is misoriented from the (001), only the centerline of the "alignment" V-groove is aligned to the  $[110]$ . The V-groove shown in Fig. 11 illustrates the case when the mask pattern is carefully aligned to the centerline. Although the mask undercut is nonuniform along the length of the V-groove (owing to the misorientation of the wafer surface from the (001)), the undercut is identical on the upper and lower edges at any given location.

More commonly, the mask pattern is not aligned to the V-groove centerline, but to one of the edges of the "alignment" V-groove. The resulting V-groove will have unequal undercuts along the two edges. Figure 12 shows the extreme left and right ends of a long V-groove (on a wafer with a misoriented (001) surface) whose mask pattern was aligned to the upper edge of a prealignment groove. The upper edge of the V-groove has a uniform undercut along the length. The lower edge has a nonuniform (and larger) undercut along the length.

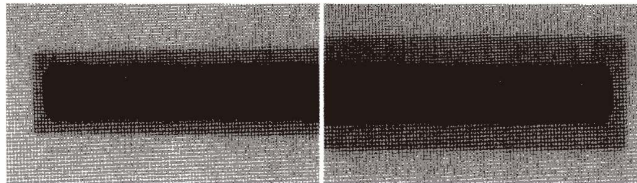


Fig. 11. V-groove etched into a wafer whose surface is misoriented from the (001). The mask pattern for this V-groove was aligned to the true  $[110]$ , defined by the centerline of a prealignment V-groove.

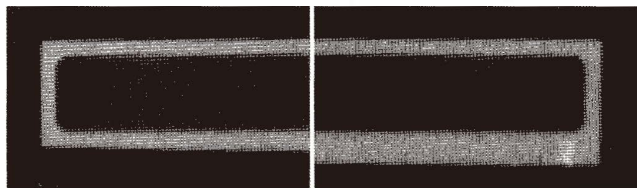


Fig. 12. V-groove etched into a wafer whose surface is misoriented from the (001). This structure differs from the V-groove in Fig. 11 in that the mask pattern was aligned to the upper edge of a prealignment V-groove rather than to the centerline.

As discussed previously, the effects of mask misalignment can be reduced by using open-ended V-groove mask patterns. In the case of wafer misorientation off the (001), the V-groove resulting from an open mask pattern can be displaced from its intended position depending on which feature of the prealignment groove (i.e., upper edge, lower edge, or centerline) the mask is aligned to. In the latter case, there will be no displacement of the centerline. Alignment of the mask to one of the edges of the prealignment groove, which is the usual procedure, will result in a shift of the centerline.

We can estimate the magnitude  $\Delta d$  of this shift as follows. A wafer whose surface is misoriented from the (001) by angle  $\alpha$  will produce a V-groove with a taper angle of approximately  $1.4\alpha$ . The one-side mask undercut rate during a Si etch in 35% KOH solution at 70°C is given by<sup>(9)</sup>

$$u = 0.545 + 0.639\theta^2, \quad (2)$$

where  $u$  is the undercut rate in  $\mu\text{m}/\text{h}$  and  $\theta$  is the misalignment angle in degrees. The centerline displacement  $\Delta d$  is proportional to half the difference in the undercut rate between the upper and lower edges. If  $t$  is the etch time in hours, the displacement is given by

$$\Delta d = 0.639 \times (1.4\alpha)^2 \times \frac{t}{2}, \quad (3)$$

where the displacement  $\Delta d$  is in microns.

This expression is plotted in Fig. 13 assuming an etch duration of 4 hours. We see that limiting the centerline displacement to  $\pm 1 \mu\text{m}$  requires the wafer orientation to be within  $\pm 0.65^\circ$  of the (001).

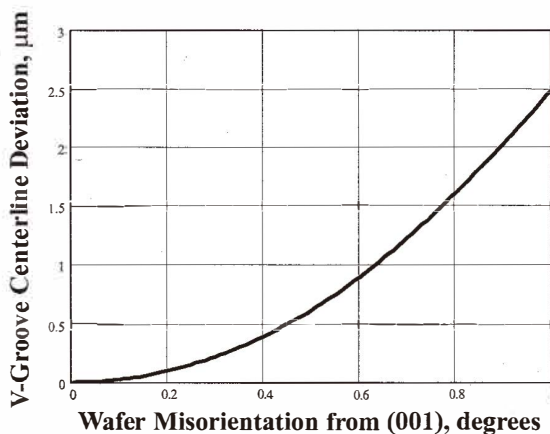


Fig. 13. V-groove centerline deviation as a function of wafer surface misorientation angle.

#### 4. Conclusions

We have experimentally demonstrated that the geometry and ultimate location of V-grooves defined by anisotropic etching of (001) silicon wafers is determined by several factors including the nature of the mask pattern, misalignment of the mask pattern to the  $\langle 110 \rangle$ , and misorientation of the wafer surface to the (001). Mask patterns with closed ends result in V-grooves whose sides are true (111) planes after long etches; open-ended mask patterns result in V-grooves with near (111) planes. Misalignment of closed-end mask patterns to the wafer  $\langle 110 \rangle$  will cause a twist of the resulting V-groove. V-grooves etched using open-end masks do not suffer from this effect. V-grooves in wafers whose surfaces are misoriented to the (001) will have nonuniform depths along the length, and can also have twisted centerlines.

#### Acknowledgments

The authors wish to thank Jasper Nijdam, John Bean, Grant Ancarrow, and Whye-Kei Lye for helpful comments.

#### References

- 1 C. A. Armiento, M. J. Tabasky, J. Chirravuri, M. A. Rothman, A. N. M. M. Choudhury, A. J. Negri, A. J. Budman, T. W. Fitzgerald, V. J. Barry and P. O. Haugsjaa: SPIE Proceedings **1582** (1991) p. 112.
- 2 A. Goto, S. Nakamura, K. Kurata, K. Komatsu and S. Ishikawa: IEEE Transactions on Components Packaging & Manufacturing Technology B **21** (1998) 140.
- 3 M. Vangbo and Y. Backlund: Journal of Micromechanics and Microengineering **6** (1996) 279.
- 4 A. J. Nijdam, E. van Veenendaal, H. Cuppen, J. van Suchtelen, M. L. Reed, J. G. E. Gardeniers, W. J. P. van Enckevort, E. Vlieg and M. Elwenspoek: Journal of Applied Physics **89** (2001) 4113.
- 5 M. Elwenspoek: Journal of the Electrochemical Society **140** (1993) 2075.
- 6 R. Wiesendanger *et al.*: Europhysics Letters **12** (1990) 57.
- 7 M. Shikida, K. Tokoro, D. Uchikawa and K. Sato: Journal of Micromechanics and Microengineering **10** (2000) 522.
- 8 Semiconductor Equipment and Materials International (SEMI), "Specifications for polished monocrystalline silicon wafers," SEMI Standard M1.15-0302, 2002.
- 9 S. Tan, R. Boudreau and M. L. Reed: Sensors and Materials **13** (2001) 303.